



## RESEARCH ARTICLE

10.1029/2018JB016190

## Crustal Structure and Dynamics of Botswana

Islam Fadel<sup>1,2</sup> , Mark van der Meijde<sup>1</sup> , and Hanneke Paulssen<sup>3</sup> <sup>1</sup>Department of Earth System Analysis, University of Twente, Enschede, Netherlands, <sup>2</sup>Geology Department, Faculty of Science, Helwan University, Helwan, Egypt, <sup>3</sup>Department of Earth Sciences, Utrecht University, Utrecht, Netherlands

## Key Points:

- The first nationwide crustal thickness and Vp/Vs ratio maps of Botswana are obtained from receiver functions
- High Vp/Vs ratios underneath the northwestern Kaapvaal Craton suggest a subsurface extension of the Bushveld mafic complex
- A thin crust and high Vp/Vs ratio are observed underneath the Passarge Basin

## Supporting Information:

- Supporting Information S1

## Correspondence to:

I. Fadel,  
i.e.a.m.fadel@gmail.com

## Citation:

Fadel, I., van der Meijde, M., & Paulssen, H. (2018). Crustal structure and dynamics of Botswana. *Journal of Geophysical Research: Solid Earth*, 123. <https://doi.org/10.1029/2018JB016190>

Received 7 JUN 2018

Accepted 7 SEP 2018

Accepted article online 13 SEP 2018

©2018. The Authors.

This is an open access article under the terms of the Creative Commons Attribution-NonCommercial-NoDerivs License, which permits use and distribution in any medium, provided the original work is properly cited, the use is non-commercial and no modifications or adaptations are made.

**Abstract** We present the first nationwide crustal thickness and Vp/Vs maps for Botswana based on the analysis of new *P* wave receiver functions of NARS-Botswana network integrated with previous receiver function results in Botswana. Using H-K analysis, we found crustal thickness values ranging from 34 km for the Okavango Rift Zone to 49 km at the border between the Magondi Belt and the Zimbabwe Craton. For stations with significant sediment cover, a sediment correction was applied based on sequential H-K stacking. We observed distinct differences for the Kaapvaal craton. The eastern part has a high Vp/Vs ratio typical of a predominantly mafic composition, suggesting lateral extension of the Bushveld mafic complex. On the other hand, the western part with a Vp/Vs ratio of 1.67 is felsic, probably as a result of delamination caused by Proterozoic rifting processes. Further to the west of the Kaapvaal Craton, we found a crustal thickness of 42 km and a Vp/Vs ratio of 1.76 for the Nosop Basin. These values are similar to other cratonic regions in Botswana, suggesting the presence of a buried craton as proposed by previous studies. We confirm a relatively thin crust (~34–39 km), compared to the rest of Botswana, and high Vp/Vs ratio (~1.84) underneath the Okavango Rift Zone found by previous receiver function studies. Notably, we also found a relatively thin crust (37 km) and high Vp/Vs ratio (1.84) in central Botswana underneath the Passarge Basin.

## 1. Introduction

The crustal structure in southern Africa mainly consists of cratons with mobile belts in between. The detailed structure of crust and upper mantle is still unknown due to limited seismic station coverage in large parts of southern Africa, in particular, in Botswana. Botswana covers three main cratonic provinces: the Kaapvaal Craton in the south and southeast, the Zimbabwe Craton in the east and northeast, and the Congo Craton in the northwest. Little is known about the extent of these cratons and the structure and geodynamical role of the mobile belts in between.

To date, only a limited number of studies (e.g., Adams & Nyblade, 2011; Kgaswane et al., 2009; Li, 2011; Nair et al., 2006; Nguuri et al., 2001; Stankiewicz et al., 2002; Yang et al., 2008; Youssef et al., 2015) investigated the crust in the southeastern part of Botswana based on data from the Southern African Seismic Experiment (SASE) temporary seismological network (Carlson et al., 1996). Recently, a new temporary seismic line was deployed across the Okavango Rift Zone (ORZ) as part of the Seismic Arrays for African Rift Initiation (SAFARI; Gao et al., 2013). Partly overlapping with these studies are some studies using other geophysical techniques: (1) deep seismic profiling for the Nosop Basin (Wright & Hall, 1990), (2) gravity and magnetic field data analysis (Corner et al., 2012; Hutchins & Reeves, 1980; Leseane et al., 2015), (3) magnetotelluric from the recent Southern African Magnetotelluric Experiment in the northern (Miensopust et al., 2011; D. Khoza, 2013; T. D. Khoza, 2013), and southwestern (Muller et al., 2009) part of Botswana, and (4) joint interpretation of magnetotelluric and seismic data (A. G. Jones et al., 2013).

From November 2013 to February 2018, a temporary array of seismometers was deployed in Botswana. This Network of Autonomously Recording Seismographs in Botswana (NARS-Botswana) network (NARS-Website, 2017) consists of 21 broadband seismic stations distributed over the whole country. It strategically covers the different geological and tectonic units and complements the existing stations MAUN from AfricaArray (AA), and LBTB from the Global Seismic Network (GSN; Figure 1). It fills a gap in station coverage for southern Africa, extending both westward and southward from previous temporary seismic deployments in Zambia, Zimbabwe, and South Africa. In this study, we will present crustal thicknesses and Vp/Vs ratios for Botswana using receiver function analysis from the new data delivered by the NARS-Botswana network and link the

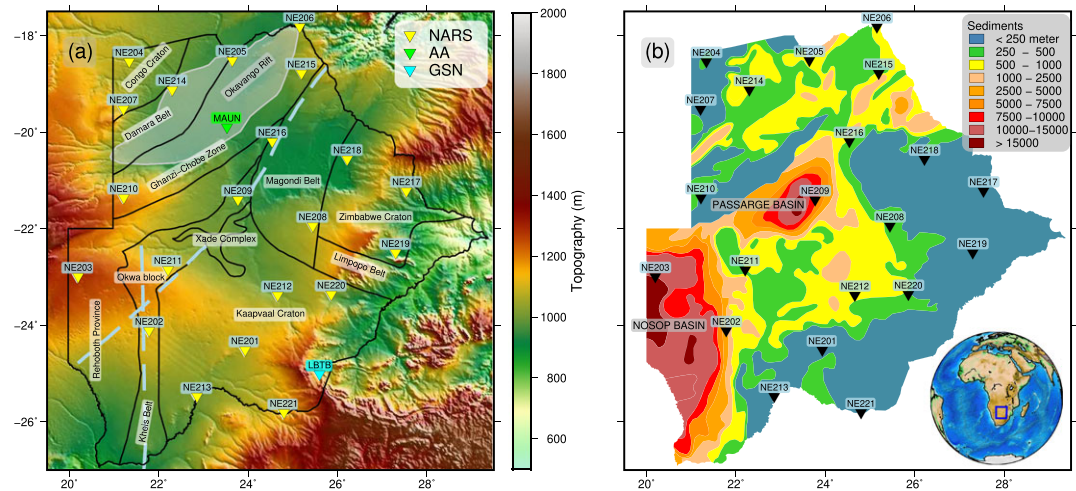


**Figure 1.** (a) An overview of the NARS-Botswana network. The black lines indicate the tectonic boundaries after Singletary et al. (2003) and McCourt et al. (2013). The yellow triangles are NARS stations used in this research, blue is GSN station LBTB, and green is AA station MAUN. The gray transparent contour outlines the Okavango Rift Zone after Yu, Liu, Reed, et al. (2015). The two light blue dashed lines comprise the Kalahari Suture Zone (KSZ) after Haddon (2005). (b) Sedimentary thickness map inferred from aeromagnetic data (modified from Pretorius, 1984) with the NARS stations on top as black triangles. NARS-Botswana = Network of Autonomously Recording Seismographs in Botswana; GSN = Global Seismic Network; AA = AfricaArray Seismological Network.

results to the geodynamics of the regions, with particular focus on the relation between cratons and mobile belts and the possible existence of rifting in the central part of Botswana.

## 2. Botswana Geological and Tectonic History

The crust of Botswana encompasses diverse tectonic features (Figure 1) with a mix of cratons and mobile belts. The cratonic areas cover the Archean Kalahari Craton with the Kaapvaal and Zimbabwe cratonic blocks in the south and east of the country and the Congo Craton in the northwest.

In between the cratonic blocks, a series of mobile belts is found: the Limpopo, Kheis-Okwa-Magondi, and Damara belts (Key & Ayres, 2000). The late Archean Limpopo Belt, reworked during the Proterozoic, is located in the east of Botswana and sutures the Kaapvaal and Zimbabwe cratons (Barton et al., 2006; Begg et al., 2009). The largest belt is the composite Kheis-Okwa-Magondi Belt that is bounded by the Kalahari Suture Zone (KSZ), which runs from southwest to northeast Botswana. The KSZ is a Paleoproterozoic major thrust zone that separates the Archean blocks to its southeast (Kalahari Craton, Zimbabwe Craton, Limpopo and Kheis-Okwa-Magondi belts) from the Proterozoic Damara, Rehoboth, and Ghanzi-Chobe belts toward the north and west (Reeves, 1978). The Damara Belt is a complex, Neoproterozoic belt that bounds the southeastern margin of the Congo Craton. It consists of a succession of metasediments that are highly deformed and metamorphosed during the Pan-African Orogeny (Haddon, 2005; Key & Ayres, 2000; Wright & Hall, 1990). Bounding the Damara Belt toward the southeast is the Ghanzi-Chobe Zone that consists of tightly folded metasediment sequences (Wright & Hall, 1990). At the northern tip, cutting across the Damara Belt and Ghanzi-Chobe Zone, is the incipient Okavango Rift, often considered to be the southwestern terminus of the East African Rift System (e.g., Leseane et al., 2015; Yu et al., 2017, and references therein).

On top of these complex and heterogeneous tectonic units, two deep sedimentary basins exist. At the center of Botswana, the Passarge basin has up to 15-km-thick Ghanzi Group sediments, which were deposited during Neoproterozoic and early Paleozoic times (Pretorius, 1984). One of the poorer-defined regions is the Rehoboth Province which extends from southwestern Botswana to western Namibia (Begg et al., 2009; van Schijndel et al., 2014). A significant part of the province aggregated around an Archean nucleus during the Paleoproterozoic (Van Schijndel et al., 2011). In the southwest, the upper part of the crust is formed by the Nosop basin. It is filled with thick Nama Group and Ghanzi Group sediments that reach up to 15-km-depth (Pretorius, 1984; Wright & Hall, 1990). Underneath it, an ancient microcraton (the Maltahohe craton) may exist (Begg et al., 2009), but it has also been interpreted as an extension of the Kaapvaal Craton (Wright & Hall, 1990).

Further details on the tectonic evolution and composition of the crust for each of the provinces are provided with the findings of crustal thickness and Vp/Vs ratio in section 4.

### 3. Data and Methods

#### 3.1. Data

NARS-Botswana is a temporary seismological network consisting of 21 broadband stations deployed across Botswana (Figure 1). The main aim of the project is to image the crustal and upper mantle structure (for more information about the NARS seismological network, the reader is referred to the NARS-Website, 2017). In this study, we used data collected from these stations, between November 2013 and August 2016, as well as from GSN station LBTB and AA station MAUN. The reader is referred to Figure S1 in the supporting information for an overview of the data used in this study.

#### 3.2. Receiver Functions

*P* wave receiver functions (RFs) are time series that contain converted *P*-to-*S* conversions from discontinuities under a seismic station. They are mainly used for estimating the crustal thickness and velocity relations Vp/Vs ratios. Crustal thickness and Vp/Vs ratio are crucial parameters for understanding the tectonic evolution, geodynamical processes and composition of the crust. RFs are derived from earthquake records at a seismic station by deconvolving the vertical component from its radial and transverse components. This, theoretically, removes both the instrument response and source imprint from the recorded signal. The remaining signal contains the direct *P* phase and *P*-to-*S* conversions at discontinuous structure underneath the station, and the corresponding reverberations (Ammon & Randall, 1990; van der Meijde et al., 2003).

In this study, *P* wave receiver functions were calculated for each station. Earthquakes with epicentral distances of 30–105° and magnitudes  $\geq 5.5$  were used. The earthquake signals were windowed between –30 to +120 s relative to the *P* wave arrival time. The theoretical arrival time was determined using the IASP91 reference model (Kennett & Engdahl, 1991). Then, the data was filtered using a Butterworth band-pass filter with corner frequencies of 0.05 and 1.25 Hz. For high-frequency RFs, used for sedimentary thickness estimation as described later, the corner frequency limits were set at 0.05 and 2.5 Hz. After that the data were rotated to radial and transverse components. Finally, the rotated components were deconvolved with the vertical one using a time domain iterative deconvolution (Ligorria & Ammon, 1999). In the deconvolution process a further Gaussian filter is applied using Gaussian width of 1.0, which acts as a low-pass filter (Ligorria & Ammon, 1999). For high-frequency RFs, used for sedimentary thickness estimation as described later, we applied different Gaussian widths of 2.5 and 5.0, corresponding to the previously used low-pass cutoffs of roughly 1.25 and 2.5 Hz, respectively.

The receiver functions were then quality controlled, passing through three tests. First, a least squares misfit criterion was used to judge the quality of the RFs, where for each event the radial RF was convolved with the vertical component to retrieve the original radial one. If the retrieved signal has at least an 85% fit with the original, the RF was considered for further processing. Second, RFs with signal-to-noise ratio (S/N) larger than 3.0 were selected, where the S/N ratio was calculated using

$$S = |A_r|/|A_t| \quad (1)$$

where  $A_r$  is the maximum amplitude on the radial RF and  $A_t$  is the maximum amplitude on the transverse RF. Finally, a visual check was done to ensure the quality of the RFs and to exclude the ones with weak or anomalous first *P* wave arrivals.

#### 3.3. H-K Analysis

H-K stacking is a well-established technique to obtain estimates of the Moho depth and Vp/Vs ratio of the crust using RFs (Zhu & Kanamori, 2000). The technique is based on searching the parameter space of all possible combinations of crustal thickness (H) and Vp/Vs ratio (K) within predefined ranges to find the maximum value of the following objective function:

$$S(H, K) = \sum_{j=1}^N w_1 r_j(t_1) + w_2 r_j(t_2) - w_3 r_j(t_3) \quad (2)$$

where  $N$  is the number of RFs at each station,  $r_j(t)$  is the amplitude function at time  $t$  of the  $j$ th RF,  $t_1$ ,  $t_2$ , and  $t_3$  are the travel times of the Moho converted phases *Ps*, *PpPs*, and *PsPs* + *PpSs* calculated for the given values of

H and K, and  $w_j$  are the weights of the three phases where  $w_1 + w_2 + w_3 = 1$ . Full details of this method can be found in Zhu and Kanamori (2000). The travel time calculations of the different converted phases require an average Vp velocity for the crust. In this study, Vp = 6.5 km/s was used based on Durrheim and Green (1992).

In this research, the H-K method searched depth intervals between 20- and 60-km depth with 0.2-km increments and Vp/Vs ratios between 1.65 and 1.95 with 0.0025 increments. The weights used were  $w_1 = 0.6$  for Ps,  $w_2 = 0.3$  for PpPs, and  $w_3 = 0.1$  for the PsPs + PpSs phases. However, for some stations, different weights ( $w_1 = 0.6$ ,  $w_2 = 0.2$ , and  $w_3 = 0.2$  or  $w_1 = 0.7$ ,  $w_2 = 0.3$ , and  $w_3 = 0.0$ ) were used based on the clarity of the Moho reverberations of the signal (for details see Table S1 in the supporting information). For the H-K analysis, RFs with Gaussian width of 1.0 were used.

In a few cases, an apparent delay of the first P arrival, due to a thick layer of sediments, was noticed. This apparently delayed first P arrival that is a composite peak of the original first P arrival combined with the direct conversion at the base of the sediment layer. For these stations we applied sequential H-K stacking (Yeck et al., 2013). It is a modified H-K stacking approach that first uses high-frequency RFs (Gaussian width = 5.0) to estimate the thickness and Vp/Vs ratio of the sedimentary layer. We assumed Vp = 3.0 km/s for the sedimentary basin, using a depth range of 0–10 km with a step size of 0.2 km, and a Vp/Vs ratio range of 1.65 to 2.7 with a step size of 0.0025. The estimated depth and Vp/Vs ratio of the sedimentary layer are then used as a correction term for a second H-K search on the RFs with Gaussian width of 2.5 to find the thickness and Vp/Vs ratio of the crust. The Gaussian width of 2.5 used for searching for the Moho in the sequential H-K analysis, instead of Gaussian width 1.0 in the case of the standard H-K analysis, is necessary to improve the discrimination between the shallow sediments and Moho reverberations. Further details on the technique can be found in Yeck et al. (2013).

Our uncertainty estimates for crustal thickness and Vp/Vs ratio are based on the approach by Youssof et al. (2013). Uncertainties are obtained by varying the Vp velocity by  $\pm 0.2$  km/s from the assumed value average crustal Vp velocity of 6.5 km/s providing upper and lower bounds of our results. It should be noted that this is a formal uncertainty corresponding to a variation in Vp velocity only. Due to complex structure, the epistemic uncertainties can be larger.

## 4. Results and Discussions

All stations in this study were subjected to conventional H-K stacking analysis. However, stations NE202, NE205, NE211, NE212, NE216, and NE220 showed a noticeable delay in the first peak (Figures 2d–2i and supporting information Figures S5, S13, S14, S18.1, and S22) that required sequential H-K analysis. Nevertheless, only for stations NE202, NE205, and NE212, significantly different results were obtained, more than 1 km beyond the uncertainty margins, compared to the conventional H-K analysis. Therefore, sequential H-K results are only presented for NE202, NE205, and NE212. Figures 2a–2c shows a representative example of the receiver function analysis using the standard H-K stacking technique applied to station NE201. The modeled theoretical Ps, PpPs, and PsPs + PpSs arrival times, based on the optimum H and K values, show good agreement with the Moho conversion and reverberations on the measured receiver functions. Figure 2d–2l shows a representative example of sequential H-K analysis, applied to station NE205. The average uncertainties in crustal thickness and Vp/Vs ratio for all stations are calculated to be in the range of  $\pm 1.5$  km and  $\pm 0.02$ , respectively. The final results for all stations are given in Table 1.

In the following, the RF results are grouped by their tectonic provinces moving from the Archean Cratonic blocks to the Archean and Proterozoic mobile belts and ending by the late Proterozoic and Phanerozoic sedimentary basins. This classification agrees with the spatial distribution of the tectonic units, where the cratonic blocks in the east and northwest are surrounded by the mobile belts, and the sedimentary basins are caught at the center of the mobile belts. We will discuss the results by first focusing on our RF results from NARS-Botswana (Table 1 and Figures 3a and 3b) and then comparing them with the results from the SAFARI (Yu, Liu, Reed, et al., 2015) and SASE (Youssof et al., 2013) networks. Figures 3c and 3d show all available RF results.

### 4.1. Cratons

#### 4.1.1. Western Zimbabwe Craton

For NARS stations on the Zimbabwe Craton (NE217, NE218, and NE219) we found crustal thicknesses varying between 40 and 49 km and Vp/Vs ratios between 1.69 and 1.78, with the thickest crust at the northwestern tip where the craton borders the Magondi Belt (Figure 3). Previous RF studies have found that the Moho beneath

**Table 1**  
*The Results of the H-K Analysis for the Different Tectonic Regions*

Tectonic regime	Station	Crustal thickness (km)			Vp/Vs			No. of Rfs
		Lower bound	Solution	Upper bound	Lower bound	Solution	Upper bound	
Western Zimbabwe Craton	NE217	37.6	40	40.6	1.78	1.78	1.81	18
	NE218	47.2	49	50.4	1.69	1.69	1.71	21
	NE219	40.8	42	43.4	1.71	1.72	1.72	20
Northwestern Kaapvaal Craton	LBTB	40.4	42	43.8	1.73	1.75	1.75	128
	NE201	34.8	36	37.8	1.80	1.81	1.82	16
	NE212 <sup>a</sup>	37.8	39	40.6	1.74	1.74	1.76	16
	NE220	37.8	39	41.0	1.81	1.82	1.83	12
Western Kaapvaal Craton	NE213	37.4	39	40.4	1.66	1.67	1.67	24
	NE221	38.0	39	40.6	1.66	1.67	1.67	22
Congo Craton	NE204	36.8	38	39.4	1.78	1.79	1.79	27
	NE207	36.8	38	39.4	1.70	1.71	1.71	11
Magondi Belt	NE208	38.8	40	41.8	1.67	1.69	1.69	14
	NE216	36.2	37	38.4	1.75	1.75	1.75	24
Kheis Belt	NE202 <sup>a</sup>	37.4	39	40.2	1.70	1.71	1.72	20
Okwa Block	NE211	42.4	44	45.0	1.72	1.72	1.72	21
Damara Belt	NE214	42.2	44	45.2	1.72	1.73	1.73	13
Ghanzi-Chobe zone	Maun	38.8	40	41.8	1.86	1.87	1.88	18
	NE205 <sup>a</sup>	37.0	38	39.6	1.81	1.81	1.81	14
	NE206	36.6	38	39.0	1.69	1.69	1.69	20
	NE210	44.6	46	47.6	1.81	1.81	1.81	18
	NE215	33.2	34	36.0	1.72	1.74	1.74	6
Passarge Basin	NE209	36.0	37	38.2	1.82	1.84	1.84	14
Nosop Basin	NE203	41.0	42	44.2	1.75	1.76	1.76	17

<sup>a</sup>Sequential H-K analysis was performed for these stations.

undisturbed Archean cratons in southern Africa is generally sharp (James et al., 2003; Nguuri et al., 2001), with a 35–40-km-thick crust that is of felsic (Nair et al., 2006) or intermediate (Youssof et al., 2013) composition. Here we interpret the Vp/Vs ratio in terms of composition based on the crustal rock study of Holbrook et al. (1992), where low (<1.78), intermediate (1.78 < Vp/Vs < 1.81) and high Vp/Vs (> 1.81) are characteristic of felsic, intermediate, and mafic crustal rocks, respectively.

For station NE217, we found a crustal thickness of 40 km and Vp/Vs of 1.78, close to the results for the undisturbed central Zimbabwe Craton of Nguuri et al. (2001;  $H = 35\text{--}40$  km), Nair et al. (2006;  $H \approx 38$  km,  $Vp/Vs \approx 1.73$ ) and Youssof et al. (2013;  $H = 35\text{--}38$ ,  $Vp/Vs = 1.74\text{--}1.79$ ). Moving south, toward NE219, and north-west, toward NE218, the crustal thickness increases toward the Limpopo and Magondi belts, respectively.

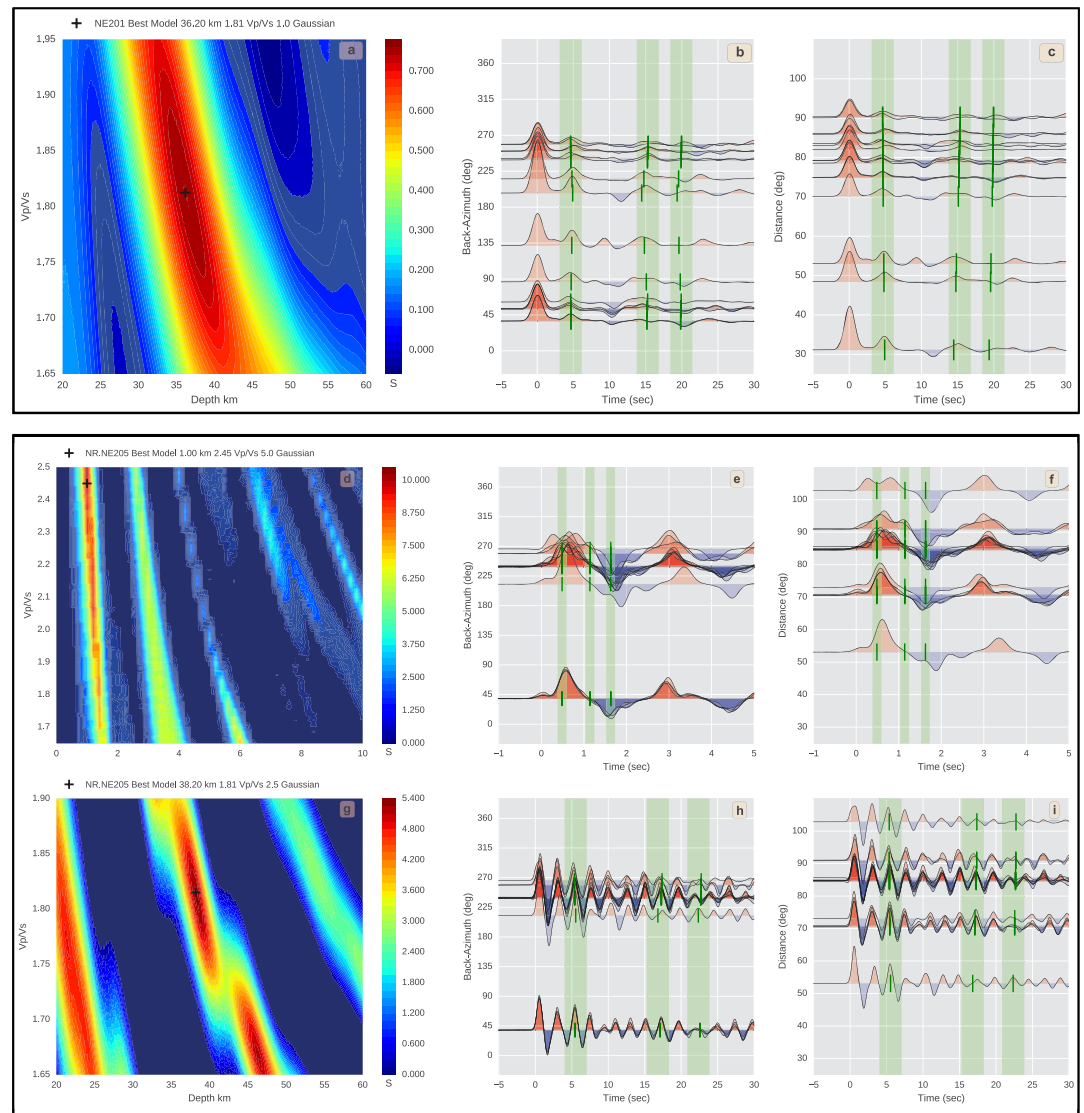


**Figure 2.** (a–c) H-K analysis for station NE201, and (d–i) sequential H-K analysis for station NE205. Figure 2a shows the H-K stacking results for station NE201, Figure 2b its receiver functions (RFs) with Gaussian width 1 ordered by back azimuth and Figure 2c ordered by epicentral distance. Figures 2d–2f present the H-K results for the sedimentary layer for station NE205 using RFs with Gaussian width of 5. Figures 2g–2i present the results for the crustal thickness using RFs with a Gaussian width of 2.5. The green lines in the RF figures indicate the times of the converted phases where  $P_s$  phase is the first,  $PpPs$  second, and  $PsPs + PpSs$  third phase to arrive. The green-shaded areas highlight the time windows of each phase.

This agrees with previous studies that have shown that post-Archean reworked belts in southern Africa have a thick crust of 45–50 km (James et al., 2003; Nguuri et al., 2001).

Station NE219 is located on the border between the Limpopo Belt and the Zimbabwe Craton. The Limpopo Belt was formed by the collision between the Zimbabwe and the Kaapvaal craton (~ 2.7 Ga; Begg et al., 2009). For NE219 we found a 42-km-thick crust, indicating a gradual increase of crustal thickness from the Zimbabwe Craton toward the Limpopo Belt (Youssof et al., 2013). The  $V_p/V_s$  value of 1.72 agrees with the values reported by Youssof et al. (2013; 1.72–1.74) and Nair et al. (2006;  $V_p/V_s \approx 1.74$ ). This confirms that the  $V_p/V_s$  values of the southern part of the Limpopo Belt are similar to those observed for undisturbed cratonic blocks.

For station NE218, on the border between the Zimbabwe Craton and the Magondi Belt, we found the largest crustal thickness among the NARS-Botswana stations and a  $V_p/V_s$  ratio of 1.69. The value of 49-km crustal thickness closely matches the 50.5 km of Youssof et al. (2013) for nearby station SA70 (Figures 3c and 3d).

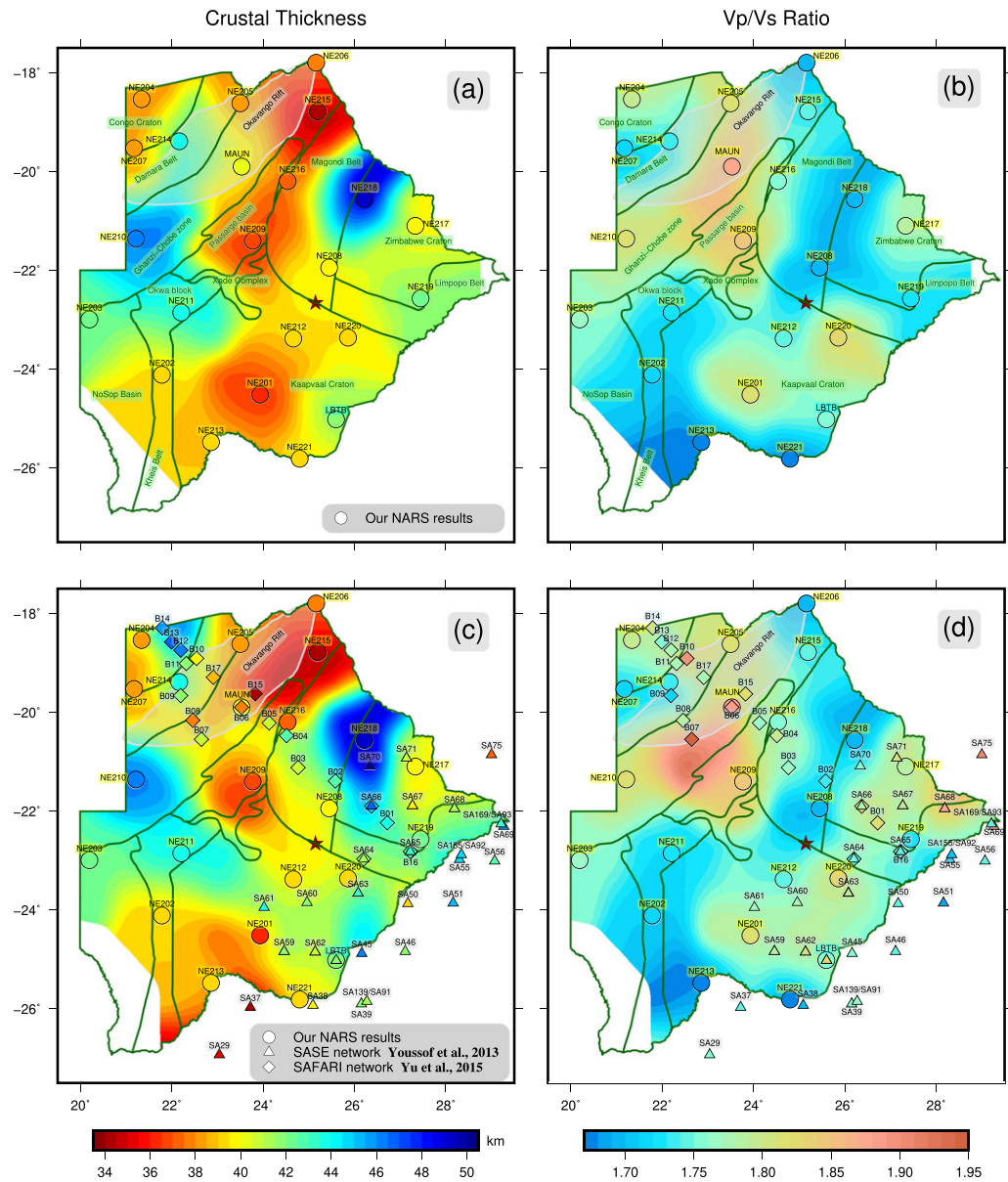


**Figure 3.** (a and b) Crustal thickness maps (km) using data from NARS stations. (c and d) Crustal thickness and Vp/Vs ratio maps using results for all RFs including Youssof et al. (2013) and Yu, Liu, Reed, et al. (2015). The dark green lines represent the tectonic boundaries presented in Figure 1a. Results from NARS-Botswana appear as circles, SASE as triangles (Youssof et al., 2013), and SAFARI as diamonds (Yu, Liu, Reed, et al., 2015). Multiple observations per location were plotted on top of each other to facilitate visual comparison. The background colored grids indicate crustal thickness and Vp/Vs ratio obtained by nearest neighbor interpolation with a search radius of 120 km, based on station distance, using Generic Mapping Tools (Wessel et al., 2013). The red star indicates the magnitude 6.5 earthquake that occurred on 3 April 2017 (USGS, 2017). NARS = Network of Autonomously Recording Seismographs; SASE = Southern African Seismic Experiment; SAFARI = Seismic Arrays for African Rift Initiation.

Nguuri et al. (2001) and James et al. (2003) explained the thick crust as a result of post-Archean reworking of the margin of the Zimbabwe Craton (~2 Ga). This reworking has produced a more complex or gradual Moho generating weak converted phases as reported by many receiver function studies (James et al., 2003; Nair et al., 2006; Nguuri et al., 2001; Youssof et al., 2013). The observed thick crust may be further affected by the collisional event between the Zimbabwe and Congo Craton during the Pan-African Damara Orogeny (Gray et al., 2008). In general, our values show a good spatial correlation with the results from the SAFARI and

SASE networks (Figure 3). However, we found a lower Vp/Vs ratio of 1.69 at NE218 than the value of 1.75 for station SA70 by Youssof et al. (2013), but it agrees with the felsic nature of the reworked belts surrounding the Zimbabwe Craton.

#### 4.1.2. Kaapvaal Craton

For the Kaapvaal Craton (stations LBTB, NE201, NE212, NE213, NE220, and NE221), we observe variations in crustal thickness between 36 and 42 km. The Vp/Vs ratios fall in two distinct blocks, suggesting different compositions. The northwestern Kaapvaal Craton block has Vp/Vs values ranging between 1.74 and 1.82, and the western Kaapvaal Craton block has Vp/Vs values of 1.67, on average (Table 1 and Figures 3a and 3b).

For the NARS stations in the northwestern part of the Kaapvaal craton (LBTB, NE201, NE212, and NE220), we found crustal thicknesses of 36–42 km and Vp/Vs ratios of 1.74–1.82 (Table 1 and Figures 3a–3c). These crustal thickness values are similar to those of the undisturbed segment of the western Zimbabwe Craton (35–40 km), although station LBTB has a slightly thicker crust of 42 km. The Vp/Vs estimates are higher than those of the undisturbed western Zimbabwe cratonic segment. The higher Vp/Vs ratio may be linked to mafic crustal intrusions as a result of the major intracratonic Bushveld intrusion event at ~2.05 Ga. The Bushveld complex is located in north central Kaapvaal Craton in South Africa with large surface outcrops. It is the largest layered mafic intrusion within the crust across the globe (Von Gruenewaldt et al., 1985). Nair et al. (2006, and references therein) proposed that this mafic intrusion may have further extended several hundred kilometers to the west. This proposed extension coincides with the location of the northwestern part of the Kaapvaal Craton in this study.

RFs of station LBTB were previously processed by Nair et al. (2006) and Youssof et al. (2013). Our results are obtained from 128 high-quality RFs from earthquakes with magnitudes > 6.0. The RFs were binned based on ray parameter between 0.04 and 0.08 s/km with a step size of 0.0025 s/km to prevent bias of the results toward specific earthquake clusters at specific distances (Figures S4.1 and S4.2 in the supporting information). Our crustal thickness estimate of 42 km agrees with Nair et al. (2006; 41.4 km) and Youssof et al. (2013; 41.5 km). However, our Vp/Vs ratio of 1.75 is significantly different from Nair et al. (2006; 1.81) and Youssof et al. (2013; 1.82). Nair et al. (2006) used only 31 RFs and Youssof et al. (2013) reported large uncertainty bounds (1.76–1.87). Our Vp/Vs result is close to the lower uncertainty bound of Youssof et al. (2013). However, we have a smaller uncertainty in our Vp/Vs estimate (1.73–1.75) due to the larger number of high-quality RFs and the binning scheme used in our study.

The stations on the western part of the Kaapvaal craton (NE213 and NE221) give a crustal thickness of 39 km and a very low Vp/Vs ratio of 1.67 (Table 1, and Figures 3a and 3b). The low Vp/Vs suggests absence of a lower crustal mafic layer due to the delamination of the lower crust and upper mantle caused by rifting during the Proterozoic (Durrheim & Green, 1992; Nair et al., 2006; Niu & James, 2002; Youssof et al., 2013). This is supported by analysis of xenolith samples from the lower crust that show a lack of mafic granulites (Schmitz & Bowring, 2003). Furthermore, Kgaswane et al. (2009) reported, based on a joint inversion of RFs and Rayleigh waves, relatively low velocities in this region, particularly in the lower part of the crust underneath station SA37 of SASE network.

#### 4.1.3. Congo Craton and Transition to Damara Belt

In the northwestern part of Botswana, two NARS stations (NE204 and NE207) are located at, or close to, the border of the Congo Craton according to the tectonic interpretation of Singletary et al. (2003; Figure 1). Both of these stations show a crustal thickness of 38 km, whereas the Vp/Vs ratio varies between 1.71 and 1.79. The three northernmost stations of Yu, Liu, Reed, et al. (2015; B12–B14) show a significantly thicker crust of ~46 km for the eastern edge of the Congo Craton (Figures 3c and 3d). The most likely interpretation is that these stations are probably not on the Congo Craton but fall within the reworked Damara Belt, and the thick crust can be related to the collisional event between the Congo and Kaapvaal craton during the Pan-African Damara Orogeny (Gray et al., 2008). For station NE214, in the Damara Belt at the border with the Congo Craton and the Okavango Rift region, we found a crustal thickness of 44 km and a Vp/Vs ratio of 1.73. The estimated values are comparable to the values of Yu, Liu, Reed, et al. (2015) and are indicative of a reworked belt of felsic composition (similar to that of the craton; Figures 3c and 3d). Our results show good agreement with those from Yu, Liu, Reed, et al. (2015) for station B11 (44.3 km and 1.72 for back azimuths 0–45 and 225–360°) and B09 (41.8 km and 1.71).

## 4.2. Mobile Belts

### 4.2.1. Kheis-Okwa-Magondi Belt

The Kheis-Okwa-Magondi Belt is assumed to be a Paleoproterozoic belt that was accreted on the northwestern border of the Kaapvaal Craton due to the Eburnean Orogeny (~2.0–1.8 Ga; Begg et al., 2009; Thomas et al., 1993). The Magondi basin was formed on the western border of the Zimbabwe Craton (~2.16–2.0 Ga) during an intracratonic extension that occurred during the early Proterozoic. Then, it was amalgamated during the Eburnean orogeny with the Okwa-Kheis belt to the west of the Archean blocks. After that, the margin between the Kheis province and the Kaapvaal Craton was deformed during the Kheis Orogeny (~1.75 Ga). Finally, the Kheis province was reactivated and amalgamated with the Rehoboth belt during the Kibaran orogeny ~1.2 Ga (Thomas et al., 1993).

This complex history is reflected in the results for the stations in this belt. The NARS stations NE208 and NE216 are located at the borders of the Magondi belt and give crustal thicknesses of 37–40 km and Vp/Vs ratios of 1.69–1.75 (Table 1 and Figures 3a and 3b). The Vp/Vs values are close to the results for stations B02–B04 (crustal thickness 42.8–42.6 and Vp/Vs 1.73–1.79) from Yu, Liu, Reed, et al. (2015) and are possibly linked to a paleocollisional zone of felsic composition (Figures 3c and 3d). However, the crustal thickness values are different, especially for stations NE216 and B04. The results from NE216 will be further discussed in section 4.3 together with station NE209 in the Passarge basin.

The RFs of the station located in the Kheis belt (NE202) required sequential H-K analysis. They showed a strong sedimentary effect (as identified by the large apparent shift of the first peak and the strong reverberation at 3 s in Figure S5 in the supporting information). This effect is particularly visible for the back azimuth range between 180 and 360° (Figures S5a–S5f in the supporting information). RF analysis for this back azimuth range did not produce coherent results and has been left out of the analysis. All results and interpretation are therefore based on RFs with 0–180 back azimuth (Figures S5g–S5l in the supporting information). Sequential H-K was applied and resulted in a sediment thickness of 0.8 km and a Vp/Vs ratio of 2.21. Finally, a crustal thickness of 39 km and Vp/Vs ratio of 1.71 were estimated using the sediment properties as time adjustment. The depth estimate did not significantly vary when we included other back azimuths. However, the Vp/Vs ratio varied significantly. This is most likely related to spatially varying sediment thickness (the station is at the border of the thick sedimentary Nosop basin, which is sampled by RFs for events with western back azimuths). The strong back azimuthal effects could not be successfully modeled, remaining for a future study when more events from various back azimuths will be available.

The Okwa Block is an isolated inlier of the Precambrian basement in the Kalahari Desert that was mapped using gravity and magnetic data of Botswana (Hutchins & Reeves, 1980). It contains the Okwa Basement Complex that crops out at the northwestern margin of the Kaapvaal Craton. Using geochronological data, Mapeo et al. (2006) showed that the Okwa Complex was emplaced rapidly around 2.056 Ga, simultaneously with the Bushveld Complex. However, the depth extension of the block was not defined due to the lack of seismological observations in this area. Station NE211 in the Okwa Block shows a relatively thick crust of 44 km and a Vp/Vs ratio of 1.72 comparable to the Kheis Belt (Table 1 and Figures 3a and 3b). The slightly thicker crust can be linked to the post-Archean reworking on the boundary of the cratonic regions during the Eburian Orogeny (~2 Ga; James et al., 2003; Youssef et al., 2013).

### 4.2.2. Damara-Ghanzi-Chobe Belt

The Damara-Ghanzi-Chobe Belt formed during the Damara Orogeny, which was part of the Neoproterozoic Pan-African tectono-thermal event between ~850 and 550 Ma, due to the collision between the Kaapvaal and Congo cratons. The Okavango Rift Zone, which is considered to be an incipient rift system, is located within the Damara-Ghanzi-Chobe Belt.

The Ghanzi-Chobe Zone is a part of this composite belt. It was formed initially as a rift basin that was filled with volcano sediments that were later deformed during the Pan-African Damara Orogeny forming a fold and thrust belt (Modie, 2000). It has spatially varying crustal thickness and Vp/Vs values (Table 1 and Figures 3a and 3b). In the southwestern part, for station NE210, we find a thick crust of 46 km and a relatively high Vp/Vs ratio of 1.81. Intermediate crustal thicknesses of 38–40 km are found in the central part, for stations MAUN and NE205, with relatively high Vp/Vs ratios of 1.81–1.87 on the border of the Okavango Rift. The northeastern part of the belt is characterized by a thin crust of 34–38 km (NE206 and NE215) and the lowest Vp/Vs ratios for this belt (1.74–1.68). Together with the results from Yu, Liu, Reed, et al. (2015), we observe a high Vp/Vs ratio at the central part of the belt. This may be an indication of partial melting in the lower crust, facilitating

the rifting process and causing the noticeable earthquake activity in the Okavango rift zone as mentioned by Yu, Liu, Moidaki, et al. (2015). The presence of either hot fluids ascending from the mantle through weak lithospheric zones or melt is further supported by the shallow Curie depth of 8–15 km from 3-D inversion of magnetic data and shallow crustal thickness from gravity data inversion (Leseane et al., 2015). However, it is important to highlight that the gravity-based crustal thickness estimates from Leseane et al. (2015) are significantly different from the receiver function results of Yu, Liu, Reed, et al. (2015) at various locations. Moreover, the surface expression of the Okavango Rift Zone does not quite match the location of the low crustal thickness, the high heat flow observation from Leseane et al. (2015), and the high Vp/Vs values found for stations B07 and MAUN from Yu, Liu, Reed, et al. (2015) and in this study. This suggests that the weak zone related to incipient rifting is located southwest of the surface expression of Okavango Rift Zone. Station NE205 showed strong reverberations from sedimentary layers underneath the station. We used a sequential H-K stack to address this problem. Although we have reduced the effects of the sediments as much as possible, the actual uncertainties in our results can be higher than the (mathematically) calculated values thereby leaving room for alternative interpretation of the crustal thickness for this station.

The analysis for station MAUN, at the southern border of the Okavango Rift, deserves special attention due to strong back azimuthal RF variability. To our knowledge, two independent studies have reported crustal thickness values for this station. Using H-K stacking Kachingwe et al. (2015) found a crustal thickness of 44 km from RFs, whereas they found 38 km from a joint inversion of RFs and surface wave dispersion curves. Yu, Liu, Reed, et al. (2015) processed their RFs grouped in different back azimuths. The 0–45° together with the 225–360° back azimuths resulted in a thickness of 37.5 km and a Vp/Vs ratio of 1.88, whereas the 45–225° back azimuth range resulted in a thickness of 43.6 km with a Vp/Vs ratio of 1.85. Yu, Liu, Reed, et al. (2015) reported that the variation in the results by Kachingwe et al. (2015) is mainly due to azimuthal dependency. Our results for MAUN agree with Yu, Liu, Reed, et al. (2015) with RFs clearly showing azimuthal variations indicative of anisotropy or dipping crustal layers under the station. However, we were only able to get a reliable result for RFs from back azimuths of 180–360°, giving a crustal thickness of 40 km and a Vp/Vs ratio of 1.87 (Figures S3d–S3f in the supporting information). For back azimuths of 0–90°, we found many RFs with Ps conversions from the Moho with reversed polarities and inconsistent H-K results. The H-K analysis of all RFs provided a crustal thickness of 43 km with 1.80 Vp/Vs, but this was strongly affected by the unreliable contribution of the RFs in the 0–90° back azimuth (Figures S3a–S3c in the supporting information).

### 4.3. Sedimentary Basins

The Passarge basin covers the Ghanzi-Chobe Belt and is bordered by the KSZ in the south (Figure 1). The KSZ is a Paleoproterozoic major thrust zone related to the formation of the Kheis-Magondi Belt and separates it from the Ghanzi-Chobe Belt and the Nosop Basin (Reeves, 1978). During Neoproterozoic and early Paleozoic times (Key & Ayres, 2000), the Passarge basin was formed. The exact mechanism is still elusive and can be due to either extensional medial rift (Haddon, 2005; C. Jones, 1979; Mason, 1998) or compressional forces (Haddon, 2005; Pretorius, 1984, 1979) that resulted in significant sedimentation presently reaching a thickness of up to 15 km.

The H-K analysis of station NE209 showed two possible solutions. The first absolute maximum stacking solution shows a crust thicker than 49 km and Vp/Vs value lower than 1.65 (Figure S11.1 in the supporting information). This solution was persistent using different stacking weights. The second local maximum stacking solution shows a thin Moho of 37 km with relatively high Vp/Vs ratio of 1.84 (Figure S11.2 in the supporting information). We prefer the second solution, since the first one has an unrealistic Vp/Vs ratio. Therefore, we picked the shallower solution as the final result for NE209 (Figure S11.2 in the supporting information). However, because of the ambiguity of the solution, it is important to mention that the RF analysis may have a high uncertainty that goes beyond the formal error given in Table 1.

For station NE216 on the boundary of the Passarge basin, we initially obtained a crust thicker than 44 km and an unrealistically low Vp/Vs ratio (lower than 1.65, Figure S18.1 in the supporting information). After investigating the RFs, we found that the solution was biased due to unclear  $P_s P_s + P_p S_s$  converted phases. Therefore, we changed the weights of the Moho converted phases from (6, 3, 1) to (7, 3, 0) to obtain a stable result with a Vp/Vs ratio of 1.75 and a crustal thickness of 37 km (Figure S18.2 in the supporting information). Comparing our crustal thickness estimate for NE216 with results for the nearby SAFARI stations B03 and B05, we observe that Yu, Liu, Reed, et al. (2015) found larger crustal thicknesses with values of around 40–42 km (Figures 3c and 3d). Similarly, large variations have been observed among nearby stations in Botswana, for example, between station B10 (40 km) and B12 (46 km) on the border of Congo Craton (Yu, Liu, Reed, et al., 2015; Figures 3c

and 3d). On the other hand, the  $V_p/V_s$  ratio of 1.75 is close to, and within the uncertainty bounds of, the  $V_p/V_s$  estimates for B04 and B05 (1.76–1.79).

The relatively thin crust and high  $V_p/V_s$  ratio observed underneath the Passarge Basin (NE209) can be linked to the Karoo/Post-Karoo rift events associated with the assemblage of Pangaea and the breakup of Gondwana (early Permian up to late tertiary and recent system, Delvaux, 1989) that affected the basin and caused observable extensional features (Haddon, 2005). It has been a long debate that the East African Rift System recent extensions exploit older weak zones of the Karoo/Post-Karoo rift zones (Dixey, 1956; Fairhead & Stuart, 1982; Haddon, 2005; Lambiase, 1989). The high  $V_p/V_s$  observed may suggest that the rifting process is still under development and may be connected to the recent tertiary activities in the Okavango Rift Zone following the *Kalahari Seismicity Axis* as proposed by Reeves (1972). Another possible scenario for the relatively high  $V_p/V_s$  ratio underneath the Passarge basin is the possible extension of the Xade mafic complex under the basin (Corner et al., 2012). This explanation is less likely because it does not explain the relatively thin crust under the basin. However, due to the local nature of the RFs and the ambiguity of the modeling process of station NE209, we could not draw solid conclusions from the observations for the Passarge Basin.

The Nosop Basin in the southwest of Botswana, which covers part of the Rehoboth Province, has a thick sedimentary sequence that reaches down to 15 km (Key & Ayres, 2000; Pretorius, 1984). The Rehoboth Province has an Archean nucleus and a major part of the province was formed during the Paleoproterozoic (2.2–1.9 Ga) (Van Schijndel et al., 2011). We found a crustal thickness of 42 km and a  $V_p/V_s$  ratio of 1.76 for station NE203 in the northwestern part of the Nosop basin (Table 1 and Figures 3a and 3b). The relatively thick crust and the intermediate  $V_p/V_s$  value are similar to the observations at LBTB station in the Kaapvaal Craton suggesting a cratonic composition. A cratonic composition for this region has been proposed before but is based on two conflicting scenarios. It might be associated to the buried Maltahohe microcraton, as suggested by Begg et al. (2009) or to an extension of the Kaapvaal Craton under the basin, as suggested by Wright and Hall (1990). Although there are similarities in thickness and  $V_p/V_s$  ratio between Kaapvaal and the crust underneath the Nosop Basin (NE203), our preferred scenario is that it is a separate craton. The Kheis-Okwa Belt and western end of the Kaapvaal Craton are significantly different in composition (with very low  $V_p/V_s$  ratios around or below 1.7), thereby separating the two cratonic blocks. Moreover, the deep sediments in the Nosop Basin suggest a different geodynamic setting with significant subsidence, which is not observed on the Kaapvaal craton. Note, however, that we only have one station in the Nosop Basin and another on the border with the Kheis-Okwa Belt, and strong conclusions can therefore not be made. Regional surface wave tomography can possibly provide more evidence for either of the two scenarios.

## 5. Summary and Conclusions

We presented the first nationwide crustal thickness estimates for Botswana from receiver function analysis. We identified different tectonic regimes with significantly different crustal structures.

The cratonic regions (Kaapvaal, Zimbabwe, and Congo craton) are on average 37–42 km thick and have  $V_p/V_s$  ratios corresponding to intermediate to mafic composition, becoming more felsic toward the borders with the mobile belts. The main exception is western Kaapvaal with a  $V_p/V_s$  ratio of 1.67 that is indicative of the absence of a mafic lower crust, probably due to delamination of the lower crust and upper mantle caused by rifting in the Proterozoic as has been suggested by previous studies.

The mobile belts show an overall thicker crust with the exception of the Damara-Ghanzi-Chobe Belt, which is affected by rifting processes. The thickest crust, of 49 km, is observed at the boundary between the Magondi Belt and the Zimbabwe Craton. The highest  $V_p/V_s$  ratio, of 1.87, is found in the northeast of Botswana for station MAUN that may be associated with incipient rifting at the Okavango Rift Zone. Moreover, we found a thin crust and high  $V_p/V_s$  ratio underneath the Passarge Basin potentially related to the Karoo/Post-Karoo rift events.

The Kheis-Okwa-Magondi Belt shows variable crustal thicknesses, with 40 km for the Magondi Belt (station NE208), 44 km for the Okwa Block, and 39 km for the Kheis Belt. The  $V_p/V_s$  ratio of this composite belt has relatively small values of 1.69–1.72, characteristic of the felsic nature of the belts surrounding the Kalahari Craton. The southern part of the belt, the Kheis block, separates the western Kaapvaal Craton from another cratonic block that has been identified underneath the Nosop Basin. Previous studies suggested that this might be either an extension of the Kaapvaal craton or the so-called buried Maltahohe microcraton. Our results are more supportive of the latter theory.

## Acknowledgments

This work was supported by a grant provided by Nederlandse Organisatie voor Wetenschappelijk Onderzoek (NWO), grant ALW-GO-AO/11-30. We are deeply grateful to Arie van Wettum from Utrecht University for his great effort to install and maintain NARS-Botswana network. We also thank our colleagues at Botswana Geological Survey, especially Tarzan Kwadiba and the members of the deployment teams, for the extraordinary effort to facilitate the installation of NARS-Botswana network. Moreover, we are deeply grateful for their great help to arrange and facilitate the local logistics. We would like to thank the AfricanArray team and Andy Nyblade for information and logistic support to reinstall Maun station. NARS-Botswana data will be made publicly available through IRIS web service in the future. The data of GSN LBTB station were accessed using the IRIS web service. The receiver function SAC files can be accessed at [https://github.com/Fadell/HK\\_NARSBotswana](https://github.com/Fadell/HK_NARSBotswana). We carried out all processing using the open software code ObsPy (Beyreuther et al., 2010). The receiver functions analysis was carried out using the open software Computer Programs in Seismology (Herrmann, 2013). The maps were produced using GMT (Wessel et al., 2013). We would like to thank JGR Associate Editor Martha Savage, the reviewer Stephen S. Gao, and an anonymous reviewer for the comments that improved the manuscript.

## References

- Adams, A., & Nyblade, A. (2011). Shear wave velocity structure of the southern African upper mantle with implications for the uplift of southern Africa. *Geophysical Journal International*, *186*(2), 808–824. <https://doi.org/10.1111/j.1365-246X.2011.05072.x>
- Ammon, C. J., & Randall, G. E. (1990). On the nonuniqueness of receiver function inversions. *Journal of Geophysical Research*, *95*(B10), 15,303–15,3318. <https://doi.org/10.1029/JB095iB10p15303>
- Barton, J., Klemd, R., & Zeh, A. (2006). The Limpopo Belt: A result of Archean to Proterozoic, Turke-type orogenesis? *Geological Society of America Special Papers*, *405*, 315–332. [https://doi.org/10.1130/2006.2405\(16](https://doi.org/10.1130/2006.2405(16)
- Begg, G., Griffin, W., Natapov, L., O'Reilly, S. Y., Grand, S., O'Neill, C., et al. (2009). The lithospheric architecture of Africa: Seismic tomography, mantle petrology, and tectonic evolution. *Geosphere*, *5*(1), 23–50. <https://doi.org/10.1130/GES00179.1>
- Beyreuther, M., Barsch, R., Krischer, L., Megies, T., Behr, Y., & Wassermann, J. (2010). ObsPy: A Python toolbox for seismology. *Seismological Research Letters*, *81*(3), 530–533.
- Carlson, R. W., Grove, T. L., De Wit, M. J., & Gurney, J. J. (1996). Program to study crust and mantle of the Archean craton in southern Africa. *Eos, Transactions American Geophysical Union*, *77*(29), 273–277. <https://doi.org/10.1029/96EO00194>
- Corner, B., Verran, D., & Hildebrand, P. (2012). Geophysical interpretation of the nature and extent of the Xade Mafic Complex, Botswana. *South African Journal of Geology*, *115*(4), 485–498.
- Delvaux, D. (1989). The Karoo to recent rifting in the western branch of the East African Rift system: A bibliographical synthesis. *Musica Roy Africana central Tervuren (Belg.)*, *Département de Géologie Mineiros Rapport Annals.*, *1990*(1991), 63–83.
- Dixey, F. (1956). The East African rift system, HM Stationery Office.
- Durrheim, R. J., & Green, R. W. E. (1992). A seismic refraction investigation of the Archean Kaapvaal Craton, South Africa, using mine tremors as the energy source. *Geophysical Journal International*, *108*(3), 812–832. <https://doi.org/10.1111/j.1365-246X.1992.tb03472.x>
- Fairhead, J., & Stuart, G. (1982). The seismicity of the East African Rift system and comparison with other continental rifts. In G. Pálmason (Ed.), *Continental and Oceanic Rifts* (Vol. 8, pp. 41–61). Washington, DC: American Geophysical Union.
- Gao, S. S., Liu, K. H., Reed, C. A., Yu, Y., Massinque, B., Mdala, H., et al. (2013). Seismic arrays to study African rift initiation. *Eos, Transactions American Geophysical Union*, *94*(24), 213–214. <https://doi.org/10.1002/2013EO240002>
- Gray, D. R., Foster, D., Meert, J., Goscombe, B., Armstrong, R., Trouw, R., et al. (2008). A Damara orogen perspective on the assembly of southwestern Gondwana. *Geological Society London Special Publications*, *294*(1), 257–278.
- Haddon, I. G. (2005). The sub-Kalahari geology and tectonic evolution of the Kalahari Basin, Southern Africa (PhD thesis). Johannesburg: Faculty of Science University of the Witwatersrand.
- Herrmann, R. B. (2013). Computer programs in seismology: An evolving tool for instruction and research. *Seismological Research Letters*, *84*(6), 1081–1088.
- Holbrook, W. S., Mooney, W. D., & Christensen, N. I. (1992). The seismic velocity structure of the deep continental crust. *Continental lower crust*, *23*, 1–43.
- Hutchins, D., & Reeves, C. (1980). Regional geophysical exploration of the Kalahari in Botswana. *Tectonophysics*, *69*(3), 201–220. [https://doi.org/10.1016/0040-1951\(80\)90211-5](https://doi.org/10.1016/0040-1951(80)90211-5)
- James, D. E., Niu, F., & Rokosky, J. (2003). Crustal structure of the Kaapvaal craton and its significance for early crustal evolution. *Lithos*, *71*(2-4), 413–429. <https://doi.org/10.1016/j.lithos.2003.07.009>
- Jones, C. (1979). The reconnaissance airborne magnetic survey of Botswana: Background and followup.
- Jones, A. G., Fishwick, S., Evans, R. L., Muller, M. R., & Fullaie, J. (2013). Velocity-conductivity relations for cratonic lithosphere and their application: Example of Southern Africa. *Geochemistry, Geophysics, Geosystems*, *14*, 806–827. <https://doi.org/10.1002/ggge.20075>
- Kachingwe, M., Nyblade, A., & Julià, J. (2015). Crustal structure of Precambrian terranes in the southern African subcontinent with implications for secular variation in crustal genesis. *Geophysical Journal International*, *202*(1), 533–547. <https://doi.org/10.1093/gji/ggv136>
- Kennett, B. L. N., & Engdahl, E. R. (1991). Traveltimes for global earthquake location and phase identification. *Geophysical Journal International*, *105*(2), 429–465. <https://doi.org/10.1111/j.1365-246X.1991.tb06724.x>
- Key, R. M., & Ayres, N. (2000). The 1998 edition of the National Geological Map of Botswana. *Journal of African Earth Sciences*, *30*(3), 427–451. [https://doi.org/10.1016/S0899-5362\(00\)00030-0](https://doi.org/10.1016/S0899-5362(00)00030-0)
- Kgaswane, E. M., Nyblade, A. A., Julià, J., Dirks, P. H. G. M., Durrheim, R. J., & Pasyanos, M. E. (2009). Shear wave velocity structure of the lower crust in southern Africa: Evidence for compositional heterogeneity within Archean and Proterozoic terrains. *Journal of Geophysical Research*, *114*, B12304. <https://doi.org/10.1029/2008JB006217>
- Khoza, T. D., Jones, A. G., Muller, M. R., Evans, R. L., Miensopust, M. P., & Webb, S. J. (2013). Lithospheric structure of an Archean craton and adjacent mobile belt revealed from 2-D and 3-D inversion of magnetotelluric data: Example from southern Congo craton in northern Namibia. *Journal of Geophysical Research: Solid Earth*, *118*, 4378–4397. <https://doi.org/10.1002/jgrb.50258>
- Khoza, D., Jones, A., Muller, M., Evans, R., Webb, S., & Miensopust, M. (2013). Tectonic model of the Limpopo belt: Constraints from magnetotelluric data. *Precambrian Research*, *226*, 143–156. <https://doi.org/10.1016/j.precamres.2012.11.016>
- Lambiase, J. (1989). The framework of African rifting during the Phanerozoic. *Journal of African Earth Sciences (and the Middle East)*, *8*(2-4), 183–190.
- Leseane, K., Atekwana, E. A., Mickus, K. L., Abdelsalam, M. G., Shemang, E. M., & Atekwana, E. A. (2015). Thermal perturbations beneath the incipient Okavango Rift Zone, northwest Botswana. *Journal of Geophysical Research: Solid Earth*, *120*, 1210–1228. <https://doi.org/10.1002/2014JB011029>
- Li, A. (2011). Shear wave model of southern Africa from regional Rayleigh wave tomography with 2-D sensitivity kernels. *Geophysical Journal International*, *185*(2), 832–844. <https://doi.org/10.1111/j.1365-246X.2011.04971.x>
- Ligorria, J. P., & Ammon, C. J. (1999). Iterative deconvolution and receiver-function estimation. *Bulletin of the Seismological Society of America*, *89*(5), 1395–1400.
- Mapeo, R., Ramokate, L., Corfu, F., Davis, D., & Kampunzu, A. (2006). The Okwa basement complex, western Botswana: U-Pb zircon geochronology and implications for Eburnean processes in southern Africa. *Journal of African Earth Sciences*, *46*(3), 253–262. <https://doi.org/10.1016/j.jafrearsci.2006.05.005>
- Mason, R. (1998). Tectonic setting of the Kalahari Suture Zone in Botswana (pp. 51–54).
- McCourt, S., Armstrong, R. A., Jelsma, H., & Mapeo, R. B. M. (2013). New U-Pb SHRIMP ages from the Lubango Region, SW Angola: Insights into the Palaeoproterozoic evolution of the Angolan Shield, southern Congo Craton, Africa. *Journal of the Geological Society*, *170*(2), 353–363. <https://doi.org/10.1144/jgs2012-059>
- Miensopust, M. P., Jones, A. G., Muller, M. R., Garcia, X., & Evans, R. L. (2011). Lithospheric structures and Precambrian terrane boundaries in northeastern Botswana revealed through magnetotelluric profiling as part of the Southern African Magnetotelluric Experiment. *Journal of Geophysical Research*, *116*, B02401. <https://doi.org/10.1029/2010JB007740>

- Modie, B. N. (2000). Geology and mineralisation in the Meso- to Neoproterozoic Ghanzi-Chobe belt of northwest Botswana. *Journal of African Earth Sciences*, 30(3), 467–474. [https://doi.org/10.1016/S0899-5362\(00\)00032-4](https://doi.org/10.1016/S0899-5362(00)00032-4)
- Muller, M., Jones, A., Evans, R., Grütter, H., Hatton, C., Garcia, X., et al. (2009). Lithospheric structure, evolution and diamond prospectivity of the Rehoboth Terrane and western Kaapvaal Craton, southern Africa: Constraints from broadband magnetotellurics. *Lithos*, 112, 93–105. <https://doi.org/10.1016/j.lithos.2009.06.023>
- NARS-Website (2017). Network of Autonomously Recording Seismographs (NARS). Retrieved from <http://www.geo.uu.nl/Research/Seismology/nars.html>
- Nair, S. K., Gao, S. S., Liu, K. H., & Silver, P. G. (2006). Southern African crustal evolution and composition: Constraints from receiver function studies. *Journal of Geophysical Research*, 111, B02304. <https://doi.org/10.1029/2005JB003802>
- Nguuri, T. K., Gore, J., James, D. E., Webb, S. J., Wright, C., Zengeni, T. G., et al. (2001). Crustal structure beneath southern Africa and its implications for the formation and evolution of the Kaapvaal and Zimbabwe cratons. *Geophysical Research Letters*, 28(13), 2501–2504. <https://doi.org/10.1029/2000GL012587>
- Niu, F., & James, D. E. (2002). Fine structure of the lowermost crust beneath the Kaapvaal craton and its implications for crustal formation and evolution. *Earth and Planetary Science Letters*, 200(1), 121–130. [https://doi.org/10.1016/S0012-821X\(02\)00584-8](https://doi.org/10.1016/S0012-821X(02)00584-8)
- Pretorius, D. (1979). The aeromagnetic delineation of the distribution patterns of Karroo volcanics in Botswana and consequent implications for the tectonics of the sub-continent. In *The Proceedings of a Seminar on Geophysics and the Exploration of the Kalahari, Geological Survey of Botswana Bulletin* (pp. 93–139).
- Pretorius, D. A. (1984). *The Kalahari Foreland, its marginal troughs and overthrust belts, and the regional structure of Botswana*. Johannesburg: University of the Witwatersrand.
- Reeves, C. (1972). Rifting in the Kalahari? *Nature*, 237(5350), 95.
- Reeves, C. (1978). The reconnaissance aeromagnetic survey of Botswana, 1975–1977. Final interpretation report, Terra Surveys Ltd, Botswana Geological Survey Departments (pp.1–315).
- Schmitz, M. D., & Bowring, S. A. (2003). Ultrahigh-temperature metamorphism in the lower crust during Neoproterozoic Ventersdorp rifting and magmatism, Kaapvaal Craton, southern Africa. *Geological Society of America Bulletin*, 115(5), 533–548.
- Singletary, S. J., Hanson, R. E., Martin, M. W., Crowley, J. L., Bowring, S. A., Key, R. M., et al. (2003). Geochronology of basement rocks in the Kalahari Desert, Botswana, and implications for regional Proterozoic tectonics. *Precambrian Research*, 121(1–2), 47–71. [https://doi.org/10.1016/S0301-9268\(02\)00201-2](https://doi.org/10.1016/S0301-9268(02)00201-2)
- Stankiewicz, J., Chevrot, S., van der Hilst, R. D., & de Wit, M. J. (2002). Crustal thickness, discontinuity depth, and upper mantle structure beneath southern Africa: Constraints from body wave conversions. *Physics of the Earth and Planetary Interiors*, 130(3), 235–251.
- Thomas, R., von Veh, M., & McCourt, S. (1993). The tectonic evolution of southern Africa: An overview. *Journal of African Earth Sciences*, 16(1–2), 5–24. [https://doi.org/10.1016/0899-5362\(93\)90159-N](https://doi.org/10.1016/0899-5362(93)90159-N)
- USGS (2017). M 6.5–132 km WSW of Mojabana, Botswana. Retrieved from <https://earthquake.usgs.gov/earthquakes/eventpage/us10008e3k#executive>.
- van Schijndel, V., Cornell, D. H., Frei, D., Simonsen, S. L., & Whitehouse, M. J. (2014). Crustal evolution of the Rehoboth Province from Archaean to Mesoproterozoic times: Insights from the Rehoboth Basement Inlier. *Precambrian Research*, 240, 22–36. <https://doi.org/10.1016/j.precamres.2013.10.014>
- Van Schijndel, V., Cornell, D. H., Hoffmann, K.-H., & Frei, D. (2011). Three episodes of crustal development in the Rehoboth Province, Namibia. *Geological Society London Special Publications*, 357(1), 27–47. <https://doi.org/10.1144/SP357.3>
- van der Meijde, M., van der Lee, S., & Giardini, D. (2003). Crustal structure beneath broad-band seismic stations in the Mediterranean region. *Geophysical Journal International*, 152(3), 729–739. <https://doi.org/10.1046/j.1365-246X.2003.01871.x>
- Von Gruenewaldt, G., Sharpe, M. R., & Hatton, C. J. (1985). The Bushveld Complex: Introduction and review. *Economic Geology*, 80(4), 803–812.
- Wessel, P., Smith, W., Scharroo, R., Luis, J., & Wobbe, F. (2013). Generic mapping tools: Improved version released. *Eos Transactions American Geophysical Union*, 94(45), 409–410. <https://doi.org/10.1002/2013EO450001>
- Wright, J. A., & Hall, J. (1990). Deep seismic profiling in the Nosop Basin, Botswana: Cratons, mobile belts and sedimentary basins. *Tectonophysics*, 173(1–4), 333–343. [https://doi.org/10.1016/0040-1951\(90\)90228-Z](https://doi.org/10.1016/0040-1951(90)90228-Z)
- Yang, Y., Li, A., & Ritzwoller, M. H. (2008). Crustal and uppermost mantle structure in southern Africa revealed from ambient noise and teleseismic tomography. *Geophysical Journal International*, 174(1), 235. <https://doi.org/10.1111/j.1365-246X.2008.03779.x>
- Yeck, W. L., Sheehan, A. F., & Schulte-Pelkum, V. (2013). Sequential H-K Stacking to obtain accurate crustal thicknesses beneath sedimentary basins. *Bulletin of the Seismological Society of America*, 103(3), 2142–2150. <https://doi.org/10.1785/0120120290>
- Youssof, M., Thybo, H., Artemieva, I., & Levander, A. (2013). Moho depth and crustal composition in southern Africa. *Tectonophysics*, 609, 267–287. <https://doi.org/10.1016/j.tecto.2013.09.001>
- Youssof, M., Thybo, H., Artemieva, I., & Levander, A. (2015). Upper mantle structure beneath southern African cratons from seismic finite-frequency P- and S-body wave tomography. *Earth and Planetary Science Letters*, 420, 174–186. <https://doi.org/10.1016/j.epsl.2015.01.034>
- Yu, Y., Liu, K. H., Huang, Z., Zhao, D., Reed, C. A., Moidaki, M., et al. (2017). Mantle structure beneath the incipient Okavango Rift Zone in southern Africa. *Geosphere*, 13(1), 102–111.
- Yu, Y., Liu, K., Moidaki, M., Reed, C., & Gao, S. (2015). No thermal anomalies in the mantle transition zone beneath an incipient continental rift: Evidence from the first receiver function study across the Okavango Rift Zone, Botswana. *Geophysical Journal International*, 202(2), 1407–1418. <https://doi.org/10.1093/gji/ggv229>
- Yu, Y., Liu, K. H., Reed, C. A., Moidaki, M., Mickus, K., Atekwana, E. A., et al. (2015). A joint receiver function and gravity study of crustal structure beneath the incipient Okavango Rift, Botswana. *Geophysical Research Letters*, 42, 8398–8405. <https://doi.org/10.1002/2015GL065811>
- Zhu, L., & Kanamori, H. (2000). Moho depth variation in Southern California from teleseismic receiver functions. *Journal of Geophysical Research*, 105(B2), 2969–2980. <https://doi.org/10.1029/1999JB900322>